External Josephson effect in Bose-Einstein condensates with a spin degree of freedom

Sahel Ashhab and Carlos Lobo*
Department of Physics, University of Illinois, 1110 West Green Street, Urbana, Illinois 61801
(Received 24 July 2001; published 19 July 2002)

We consider the Josephson effect between two spatially separated Bose-Einstein condensates of atoms each of which can be in two hyperfine states. We derive simple equations of motion for this system closely analogous to the Bloch equations. We also map the dynamics of the system onto those of a classical particle in a well. We find density and spin modes of oscillation and stable equilibrium points of the motion that are unstable in the spinless case. Finally we analyze the oscillation modes in the spin-1 ($F=1$) case.

DOI: 10.1103/PhysRevA.66.013609 PACS number(s): 03.75.Fi, 74.50.+r, 05.30.Jp

I. INTRODUCTION

Recent experiments on the Josephson effect in ^{3}He have uncovered phenomena that have not been previously observed in conventional superconducting junctions or in ^{4}He superleaks [1]. Some authors have attributed these effects to the spin of the Cooper pairs since they are paired in an $S=1$ configuration [2,3]. By analogy this suggests that the simple Josephson effect in Bose condensed alkali-metal gases could be qualitatively modified by the presence of an internal spin degree of freedom. Recently several experimental groups have succeeded in forming this kind of condensate in which the atoms can be in more than one hyperfine state. Myatt *et al.* [4] have trapped the $|F=2,m_F=1\rangle$ and $|F=1,m_F=-1\rangle$ states of ^{87}Rb using magnetic fields. Stamper-Kurn *et al.* [5] have trapped the $F=1$ multiplet of ^{23}Na with optical methods. An important feature of their setup is the possibility of imaging each species separately, thus allowing them to observe their individual motion. There have also been several theoretical studies of these systems [6–9].

The external Josephson effect, i.e., between two spatially separated condensates in the case of a single hyperfine state, has already been addressed extensively in the literature [10–17]. Josephson-like phenomena have been observed experimentally [18,19]. The internal Josephson effect (between hyperfine states) has also been analyzed [20]. In the present work we study only the external Josephson effect between two condensates in a double-well potential whose atoms have two possible internal states designated as $|1\rangle$ and $|2\rangle$. A weak link is established between the condensates by lowering the potential barrier that separates them.

In this paper we discuss three main results. First we show that, under certain conditions, it is possible to map the motion of the total condensate density onto that of a fictitious particle in a simple effective potential. This result is very general and it applies also to condensates without a spin degree of freedom. Second, we study the motion of another dynamical variable, related to the spin motion, and we find that, under the same conditions, it can also be mapped onto the motion of a fictitious spin precessing in a magnetic field. Finally we study the equilibrium points and show that apart from the ''trivial'' one (the lowest-energy state of the junction), there are others including some that, in the spinless case, are experimentally inaccessible.

This paper is organized as follows: First we describe the model and the Hamiltonian of the system in Sec. II. After that, in Secs. III A and III B we derive the equations of motion and show that in the so-called isotropic limit, they reduce to a form which is equivalent to the well-studied Bloch equations. We map the dynamics of density oscillations onto those of a classical particle in a well. In Sec. III C we identify the equilibrium points of the motion and study their dynamic stability. Finally, in Sec. IV we make some considerations regarding the extension to the $F=1$ case (when the trapping potentials for all three m_F sublevels are identical).

II. MODEL SYSTEM AND HAMILTONIAN

Let us take a condensate in a symmetric double-well potential where the barrier is much larger than the chemical potential and therefore, in order to go from one side to the other, the atoms must tunnel under the barrier. Each atom has two possible hyperfine states, which means that the order parameter is a two-component function. This setup can be achieved by taking a condensate in a single well and raising a potential barrier in the middle, thereby splitting it into two parts. Following this we may apply laser pulses to each side selectively in order to choose a particular superposition of the internal states of the atoms on each side.

We shall now make a four-mode approximation to describe the system. Let $|1,R\rangle$, $|2,R\rangle$, $|1,L\rangle$, and $|2,L\rangle$ be the four single-atom states corresponding to the four modes, where the labels R and L refer to the right and left wells. The single atom states are, in principle, time dependent and will be approximately given, in the adiabatic approximation, by the Gross-Pitaevskii ground state, which in turn is determined by the number of particles in each single-atom state. When each of the four states defined above is macroscopically occupied, the condensate wave function $\Psi^i_{R,L}(i=1,2)$ inside each of the wells can be well described at the Gross-Pitaevskii level.

We shall assume that the system is always in the semiclassical regime, i.e., that the fluctuations around the mean values of the physical quantities are small (see below). With this proviso we can describe the system in terms of classical (c-number) canonically conjugate variables [17]. The semi-

*Present address: Laboratoire Kasstler-Brossel, École Normale Supérieure, 24 rue Lhomond, 75231 Paris Cedex 05, France.

classical variables are: $\Delta N_i \equiv (N_{i,R} - N_{i,L})/2$, i.e., one-half of the difference in the number of atoms between the two wells in each internal state and the corresponding relative phases $\Delta\varphi_i$. Each pair of ΔN_i and $\Delta\varphi_i$ are canonically conjugate to each other. The condensate wave function can be expressed in terms of these variables as $\Psi^j_{R,L} = \sqrt{N_j \pm \Delta N_j}\exp(\pm i\Delta\varphi_j/2)$ up to an overall phase factor, where the N_j's are one-half of the total number of atoms in state j. Since we are assuming in this paper that there is no laser coupling between the different spin states, it follows that the different N_j's are conserved separately. Therefore the dynamics is not naturally described by using as variables the relative phases between internal states in each well. Although the difference in chemical potential between the two species in each well can be very large, this does not affect the Josephson dynamics. For the same reason, the dephasing between states of different hyperfine spin is irrelevant.

Furthermore, if we restrict ourselves to values of $(\Delta N_1 + \Delta N_2)/(N_1 + N_2) \ll 1$, we can write down an approximate Hamiltonian, which is the straightforward generalization of the spinless case and reduces to it when one of the N_i's (and therefore ΔN_i) goes to zero:

$$H = H_J + H_{\rm int}, \tag{1}$$

$$H_J = -\omega_0 \sum_{i=1,2} \sqrt{N_i^2 - \Delta N_i^2}\cos\Delta\varphi_i \tag{2}$$

and

$$H_{\rm int} = \frac{1}{2}(\epsilon_{11}\Delta N_1^2 + \epsilon_{22}\Delta N_2^2 + 2\epsilon_{12}\Delta N_1\Delta N_2). \tag{3}$$

H_J is the Josephson coupling Hamiltonian and $H_{\rm int}$ is the interaction Hamiltonian (for a derivation of these see [11,15]). The interaction term conserves the total number of atoms in each hyperfine state separately (we are here ignoring loss processes that occur in the real system). ω_0 is the Josephson tunneling energy, which we take to be the same for both hyperfine states for simplicity, and ϵ_{ij} are the effective interaction coefficients. We assume that ω_0 is independent of ΔN_i and $\Delta\varphi_i$, although we do expect some dependence for large values of ΔN_i. The expression for the coefficients ϵ_{ij} in terms of the density ρ_i of species i and the interaction parameter $g_{ij} = 4\pi\hbar^2 a_{ij}/m$ is

$$\epsilon_{ij} = \frac{g_{ij}}{N_i N_j}\int d\mathbf{r}\rho_i\rho_j, \tag{4}$$

where a_{ij} is the s-wave scattering length between atoms of type i and j. We assume here that the gas is very dilute ($\rho_i a_{ij}^3 \sim 10^{-5}$), which means that the mean-field approximation works extremely well.

In order to justify the the effective Hamiltonian we shall assume that all ϵ's are positive because we want to avoid two possible complications: the collapse of the gas and a possible accumulation of atoms on one side of the junction. The two components must also be miscible. In other words, there can be no component separation. If this were not the case, we might not have the same tunneling matrix element ω_0 for both species, and the mean-field interaction energy would not have the form that we assume. This means that a condition must be imposed on the interaction parameters, namely, that $\epsilon_{11}\epsilon_{22} > \epsilon_{12}^2$ [21].

In the spinless case we can identify four different dynamical regimes as the parameters ω_0 and ϵ are varied. By analyzing the topology of the phase space [Figs. 1(a)–1(c)], we find two sharp transitions and one crossover. Starting from the weakly interacting limit [the so-called Rabi regime, Fig. 1(a)] the transition to the intermediate regime is marked by the appearance of closed orbits oscillating around nonzero values of ΔN and centered at $\Delta\varphi = \pi$ [Fig. 1(b)]. The second one occurs when open orbits appear where $\Delta\varphi$ extends over all values [Fig. 1(c)]. This is a transition from the intermediate to the Josephson regimes. These transitions happen at the values $\omega_0 = \epsilon N$ and $2\omega_0 = \epsilon N$, respectively, for our model. Finally when $\omega_0 N \sim \epsilon$ there is a crossover to the Fock regime where quantum phase fluctuations cannot be neglected. Deep in the Rabi regime (when $\omega_0 \gg \epsilon N$) the tunneling energy dominates. In the Josephson regime both H_J and $H_{\rm int}$ are important ($\omega_0 \ll \epsilon N \ll \omega_0 N^2$) and finally, in the Fock regime, $H_{\rm int}$ dominates ($\omega_0 N \ll \epsilon$) [17].

Under current experimental conditions ω_0 can be varied anywhere from 0 to 100 s^{-1}. On the other hand, ϵ can go from 0.01 to 0.1 s^{-1} [15], and N is usually between 10^4 and 10^7. With this range of parameters the Fock and Josephson regimes are easily accessible, whereas the Rabi regime is more difficult to achieve. It is important that the frequency of any oscillation between the wells be smaller than the lowest intrawell excitation frequencies so that, during the motion, these degrees of freedom are not excited. In practice this means that both ω_0 and $\sqrt{\omega_0\epsilon N}$ have to be smaller than the frequency of the lowest intrawell collective mode (as will become clear below).

To be consistent with the semiclassical description we require that the standard deviations of the quantum operators $\Delta\hat{\varphi}$ and $\Delta\hat{N}$ satisfy the conditions $\sigma(\Delta\hat{\varphi}) \ll 1$ and $\sigma(\Delta\hat{N}) \ll N$ during the motion of the system. Generally speaking, the experimental setups will be such that $\sigma(\Delta\hat{N}) \sim \sigma^{-1}(\Delta\hat{\varphi}) \sim (\epsilon/\omega_0 N + 1/N^2)^{-1/4}$. The second inequality is always satisfied for positive ϵ's. The first is satisfied only in the Josephson and Rabi regimes, to which we shall restrict our analysis from now on.

Finally, the experimental observations can be made by measuring the density (and therefore $\Delta N_{1,2}$) in the usual way, either destructively or by phase-contrast imaging. As mentioned before, an important point is that these methods allow us to determine experimentally the behavior of each hyperfine species separately.

III. DYNAMICS, BLOCH EQUATIONS, AND EQUILIBRIUM POINTS

The equations of motion are

$$\dot{\Delta N_i} = -\frac{\partial H}{\partial\Delta\varphi_i} = -\omega_0\sqrt{N_i^2 - \Delta N_i^2}\sin\Delta\varphi_i, \tag{5}$$

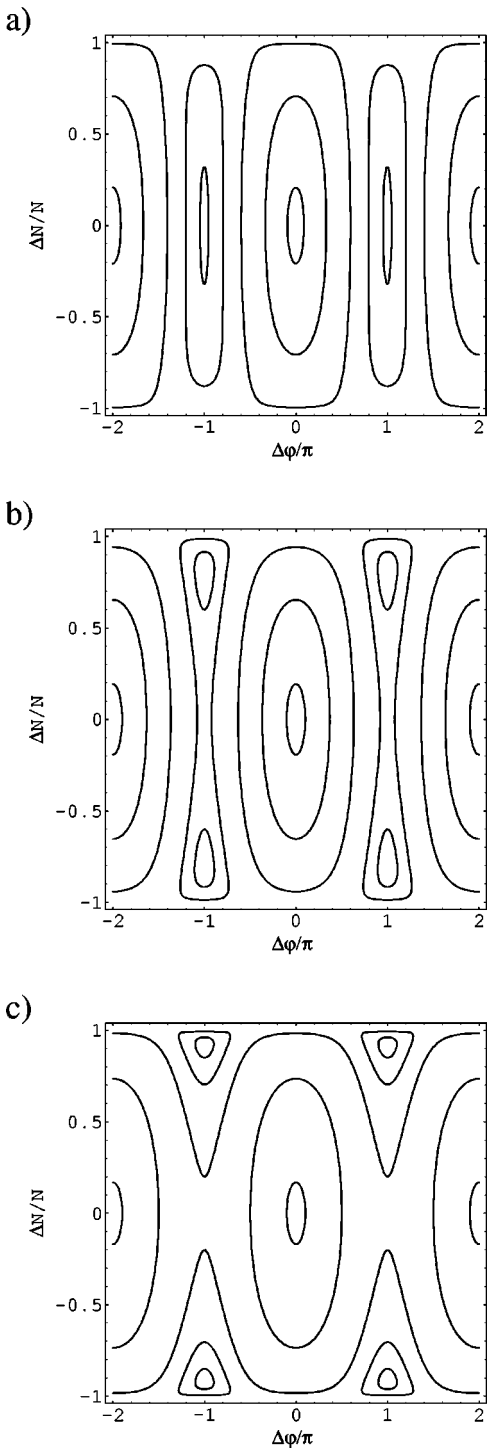

FIG. 1. Orbits in phase space of the spinless Josephson effect: (a) Rabi regime $\omega_0/\epsilon N=1.2$, (b) intermediate regime $\omega_0/\epsilon N=0.6$, (c) Josephson regime $\omega_0/\epsilon N=0.4$.

$$\dot{\Delta\varphi_i}=\frac{\partial H}{\partial \Delta N_i}$$

$$=\omega_0\frac{\Delta N_i}{\sqrt{N_i^2-\Delta N_i^2}}\cos\Delta\varphi_i+\sum_j \epsilon_{ij}\Delta N_j. \qquad (6)$$

In Secs. III A and III B we will rewrite the equations of motion in terms of new variables in order to provide some insight into the dynamics of the system.

A. Isotropic case

We first consider the isotropic case, where $\epsilon_{11}=\epsilon_{12}=\epsilon_{22}$. We shall be working with the quantity $\epsilon\equiv(\epsilon_{11}+\epsilon_{22}+2\epsilon_{12})/4$, which is in fact equal to any of the ϵ's in the isotropic case. This definition, however, will be useful ahead, when we deal with the anisotropic situation. The equality of the interaction parameters in the isotropic case seems to violate the miscibility condition that $\epsilon_{11}\epsilon_{22}>\epsilon_{12}^2$. However this condition does not take into account the kinetic energy, which favors miscibility. Therefore isotropy does not pose any such problems.

We notice that the Hamiltonian (1) is invariant under arbitrary spin rotations and more generally under SU(2) transformations applied simultaneously to the spins in both wells. That is, if we transform the two-component spinors Ψ_L and Ψ_R with the same unitary operator, the dynamics should remain unchanged. This suggests that we reexpress the equations of motion in terms of quantities that are invariant under such transformations. This conclusion of course depends on the isotropy of the interaction Hamiltonian $H_{\rm int}$. We therefore define the following dot products of spinors:

$$\Delta N_+\equiv\frac{|\Psi_R|^2-|\Psi_L|^2}{2}=\sum_i \Delta N_i, \qquad (7)$$

$$\alpha_+\equiv\frac{\Psi_L^*\Psi_R-\Psi_R^*\Psi_L}{2i}=\sum_i \sqrt{N_i^2-\Delta N_i^2}\sin\Delta\varphi_i, \qquad (8)$$

$$\beta_+\equiv\frac{\Psi_L^*\Psi_R+\Psi_R^*\Psi_L}{2}=\sum_i \sqrt{N_i^2-\Delta N_i^2}\cos\Delta\varphi_i. \qquad (9)$$

The subscript $(+)$ will be used to distinguish this set of variables from another one with subscript $(-)$ to be defined below. Using the equations of motion for ΔN_i and $\Delta\varphi_i$, we obtain

$$\begin{pmatrix}\dot{\Delta N}_+\\ \dot{\alpha}_+\\ \dot{\beta}_+\end{pmatrix}=\begin{pmatrix}0 & -\omega_0 & 0\\ \omega_0 & 0 & +\epsilon\Delta N_+\\ 0 & -\epsilon\Delta N_+ & 0\end{pmatrix}\begin{pmatrix}\Delta N_+\\ \alpha_+\\ \beta_+\end{pmatrix}. \qquad (10)$$

If we now define the three-component vectors $\mathbf{r}_+=(\Delta N_+,\alpha_+,\beta_+)$ and $\mathbf{B}(t)=(-\epsilon\Delta N_+,0,\omega_0)$, we can rewrite the equations of motion succinctly as

$$\dot{\mathbf{r}}_+=\mathbf{B}(t)\times\mathbf{r}_+. \qquad (11)$$

Note though that $\mathbf{B}$ and $\mathbf{r}_+$ are not independent since they are both functions of ΔN_+.

Straightforward manipulation of Eq. (10), or directly of Eqs. (5) and (6), leads to

$$\ddot{\Delta N}_+=-[\omega_0^2-\epsilon H(0)]\Delta N_+-\frac{\epsilon^2}{2}\Delta N_+^3, \qquad (12)$$

where $H(0) = -\omega_0 \beta_+(0) + (\epsilon/2)\Delta N_+(0)^2$.

This equation is quite general since it is valid not only for two hyperfine states but for any number of them, as long as they interact only through a $\Delta N_+^2 \equiv (\Sigma_i \Delta N_i)^2$ term. In particular, it also applies to a single-state (i.e., spinless) system. It is formally identical to the equation of motion of a particle with unit mass in the quadratic-plus-quartic effective potential

$$V_{eff}(\Delta N_+) = \frac{1}{2}[\omega_0^2 - \epsilon H(0)]\Delta N_+^2 + \frac{\epsilon^2}{8}\Delta N_+^4 \qquad (13)$$

with effective total energy

$$E_{eff} = V_{eff}(\Delta N_+) + \frac{1}{2}\dot{\Delta N}_+^2 . \qquad (14)$$

An important point to notice is that E_{eff} and V_{eff} cannot be chosen independently since they both depend on the initial conditions. The variation of $H(0)$ and of $\alpha_+(0)$ (since $\dot{\Delta N}_+ = -\omega_0 \alpha_+$) allows us to find three different types of motion [Figs. 2(a–c)]. In the first type the coefficient of the quadratic term is positive and ΔN_+ oscillates around zero, which is the minimum of V_{eff} [Fig. 2(a)]. In the spinless case this corresponds to either oscillations around the origin [Figs. 1(a)–1(c)] or to small oscillations around the π state [Fig. 1(a)]. The second case occurs when the coefficient is negative and E_{eff} is positive, which also leads to oscillations of ΔN_+ around zero although that point is no longer a minimum of V_{eff} [Fig. 2(b)]. It corresponds to large oscillations around the origin or the π state [Figs. 1(b) and 1(c)]. The third one corresponds to both E_{eff} and the coefficient being negative [Fig. 2(c)] and leads to self-trapped behavior [oscillations around $\Delta N_+ \neq 0$; Figs. 1(b) and 1(c)]. For the spinless case there is a well-known analogy with a momentum-shortened pendulum in a gravitational field, whose behavior is also fully reproduced by this particle-in-a-well model. Since the analysis of the spinless junction has already been carried out in Ref. [11] we shall not continue it here and shall proceed to the two-hyperfine-state case.

Specifying the dynamics of ΔN_+ does not describe the motion completely. For example, even in the spinless case it is known that the third regime includes two different behaviors of the relative phases, the so-called ''running'' and ''oscillating'' phases. For a description of these as well as π states and the momentum-shortened pendulum analogy see, e.g., Ref. [11]. To further understand the dynamics of the two-hyperfine-state Josephson effect we introduce the additional variables

$$\Delta N_- \equiv \Delta N_1 - \Delta N_2, \qquad (15)$$

$$\alpha_- \equiv \sqrt{N_1^2 - \Delta N_1^2}\sin\Delta\varphi_1 - \sqrt{N_2^2 - \Delta N_2^2}\sin\Delta\varphi_2, \quad (16)$$

$$\beta_- \equiv \sqrt{N_1^2 - \Delta N_1^2}\cos\Delta\varphi_1 - \sqrt{N_2^2 - \Delta N_2^2}\cos\Delta\varphi_2, \quad (17)$$

and their equations of motion are

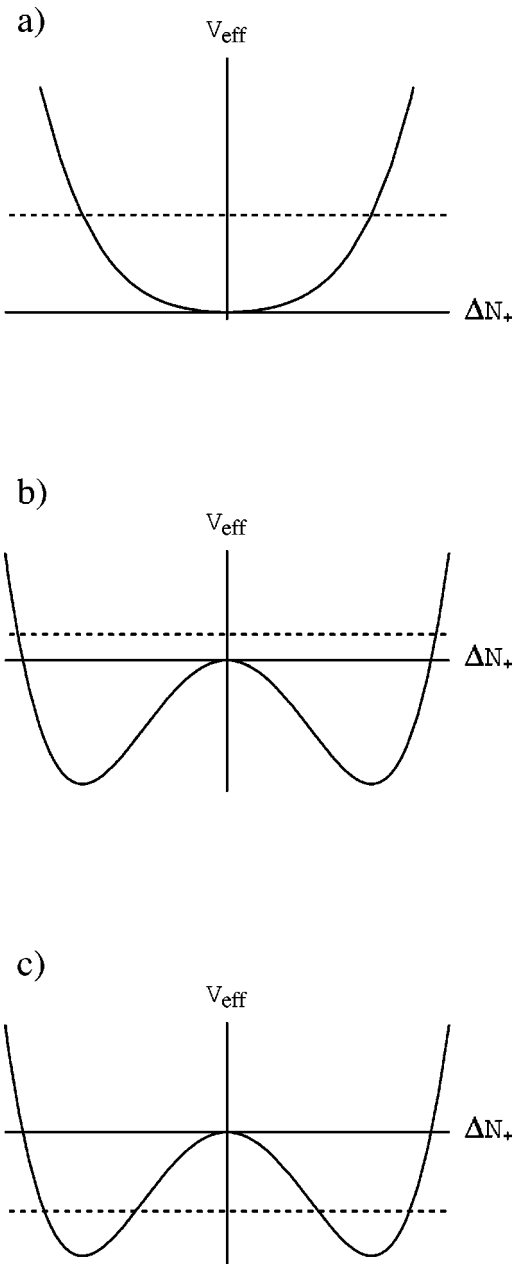

FIG. 2. $V_{eff}(\Delta N_+)$ for different initial conditions: (a) when the coefficient of the quadratic term in Eq. (13), namely, $\frac{1}{2}\omega_0^2 - \epsilon H(0)$, is positive; (b) when the coefficient is negative and $E_{eff} > 0$; (c) when both the coefficient and E_{eff} are negative. The horizontal line corresponds to E_{eff}.

$$\begin{pmatrix} \dot{\Delta N}_- \\ \dot{\alpha}_- \\ \dot{\beta}_- \end{pmatrix} = \begin{pmatrix} 0 & -\omega_0 & 0 \\ \omega_0 & 0 & +\epsilon\Delta N_+ \\ 0 & -\epsilon\Delta N_+ & 0 \end{pmatrix} \begin{pmatrix} \Delta N_- \\ \alpha_- \\ \beta_- \end{pmatrix}. \qquad (18)$$

Since the matrix is the same as in Eq. (10) we define the three-component vector $\mathbf{r}_- = (\Delta N_-, \alpha_-, \beta_-)$ and rewrite the equations of motion as

$$\dot{\mathbf{r}}_- = \mathbf{B(t)} \times \mathbf{r}_-. \qquad (19)$$

TABLE I. Equilibrium points, and oscillation modes around them, in the isotropic case.

$\Delta\varphi_1,\Delta\varphi_2$	$\Delta N_1,\Delta N_2$	Existence condition	Type of mode	Frequency	Stability condition
0,0	0,0	Always exists	Density	$\sqrt{\omega_0^2+\omega_0\epsilon N}$	Always stable
			Spin	ω_0	
π,0	0,0	Always exists	Mixed	$\sqrt{\omega_0^2+\omega_0\epsilon(N_2-N_1)}$	$N_1-N_2-\omega_0/\epsilon<0$
			Spin	ω_0	Always stable
	$\neq 0$	$N_1-N_2-\omega_0/\epsilon>0$	Mixed	$\epsilon\lvert\Delta N_+^0\rvert$	Always stable
			Spin	$\sqrt{\omega_0^2+\epsilon^2(\Delta N_+^0)^2}$	
π,π	0,0	Always exists	Density	$\sqrt{\omega_0^2-\omega_0\epsilon N}$	$N_1+N_2-\omega_0/\epsilon<0$
			Spin	ω_0	Always stable
	$\neq 0$	$N_1+N_2-\omega_0/\epsilon>0$	Density	$\epsilon\lvert\Delta N_+^0\rvert$	Always stable
			spin	$\sqrt{\omega_0^2+\epsilon^2(\Delta N_+^0)^2}$	

Now, however, $\mathbf{B}$ and $\mathbf{r}_-$ are independent and therefore these equations are formally identical to the Bloch equations (without any relaxation terms), familiar from the context of nuclear magnetic resonance and quantum optics. Notice that in going from the original four variables to six we are enlarging the configuration space, which means that not all points described by the new set of variables are physically allowed. Therefore care must be taken in choosing the initial conditions of the motion.

We can obtain some physical insight into the variables $\Delta N_\pm$ by noting that ΔN_+ is one-half of the difference in total number between the right and left wells and ΔN_- is one half of the difference in the z component of spin between the wells $(|\Psi_R^1|^2-|\Psi_R^2|^2)/2-(|\Psi_L^1|^2-|\Psi_L^2|^2)/2$. This means that the former describes the density mode whereas the latter, in that limit, describes the spin mode.

We can now analyze Eqs. (11) and (19) in a few limiting cases to gain some insight into the behavior of the system. Under appropriate conditions it is possible to have small oscillations in ΔN_+ and no motion in ΔN_- or vice versa. We consider two cases: the Rabi limit, where $\epsilon N \ll \omega_0$, and the Josephson regime, where $\epsilon N \gg \omega_0$. In the Rabi case, neglecting higher-order terms, the frequency of oscillation of ΔN_+ (and therefore of the density mode) can be calculated from Eq. (13) to be $\sqrt{\omega_0^2+\omega_0\epsilon\beta_+}$. Also, using Eq. (19), we can neglect the component of the $\mathbf{B}$ field along the ΔN_- axis, so that $\mathbf{r}_-$ (the spin mode) rotates around the β_- axis with frequency ω_0. In the Josephson case we consider two types of situations—small oscillations of ΔN_+ around zero and around nonzero values. For zero values we get density and spin modes with frequencies $\sqrt{\omega_0^2+\omega_0\epsilon N}$ and ω_0, respectively. For nonzero values (i.e., when ΔN_+ is "self-trapped" around a value ΔN_+^0), ΔN_+ oscillates with frequency $\epsilon\lvert\Delta N_+^0\rvert$ and ΔN_- oscillates with frequency $\sqrt{\omega_0^2+\epsilon^2(\Delta N_+^0)^2}$. In Sec. III C we shall treat special cases of the above results using a different method that applies in the limit of small oscillations.

B. Anisotropic case

As we would expect, the equations in this case become much more complicated. However, for the sake of completeness, we include them here. We find that the equations for $\dot{\mathbf{r}}_+$ and $\dot{\mathbf{r}}_-$ become coupled:

$$\dot{\mathbf{r}}_+ = \mathbf{B_1}(t)\times\mathbf{r}_+ + \mathbf{B_2}(t)\times\mathbf{r}_-, \tag{20}$$

$$\dot{\mathbf{r}}_- = \mathbf{B_1}(t)\times\mathbf{r}_- + \mathbf{B_2}(t)\times\mathbf{r}_+, \tag{21}$$

where $\mathbf{B}_1=(-\epsilon\Delta N_+-\epsilon_B\Delta N_-,0,\omega_0)$, $\mathbf{B}_2=(-\epsilon_A\Delta N_- -\epsilon_B\Delta N_+,0,0)$, $\epsilon\equiv\frac{1}{4}(\epsilon_{11}+\epsilon_{22}+2\epsilon_{12})$ as before, $\epsilon_A\equiv\frac{1}{4}(\epsilon_{11}+\epsilon_{22}-2\epsilon_{12})$ and $\epsilon_B\equiv\frac{1}{4}(\epsilon_{11}-\epsilon_{22})$.

C. Discussion of the equilibrium points of the motion

In this section we study the existence and stability of the equilibrium points of motion. To do this we can use the equations derived in the preceding section. However we will work directly with Eqs. (5) and (6) since it turns out that they are more intuitive for our purposes. The detailed calculations are done in the Appendix and the main results for the isotropic case are summarized in Table I.

As can be expected, the lowest-energy state is characterized by $\Delta\varphi_{1,2}=\Delta N_{1,2}=0$. The density and spin modes of oscillation around that equilibrium point can also be understood in a simple way as in and out of phase oscillations of two coupled Josephson currents. The condition of stability of the π states ($\Delta\varphi_1=\pi$ and $\Delta\varphi_2=0$) can be satisfied by controlling the number of atoms in the two components $N_{1,2}$. This means that the stability of π states in spinor condensates is robust regardless of the ratio ω/ϵ. As far as self-trapped equilibrium points are concerned, we find two stable ones. In the case of the $\Delta\varphi_1=\pi$, $\Delta\varphi_2=0$ state, the two components are self-trapped on opposite sides of the junction, whereas in the case of $\Delta\varphi_1=\Delta\varphi_2=\pi$ the two components are self-trapped on the same side. However, as we will see below, for typical experimental parameters, these states are outside of the region of validity of the Gross-Pitaevskii (mean-field) description.

D. Experimental considerations

The typical frequencies of small oscillations can be calculated using the following parameters: $N\sim 10^6$ atoms, $\epsilon\sim 0.01\ \mathrm{s}^{-1}$, $\epsilon_{A,B}\sim 10^{-4}\ \mathrm{s}^{-1}$, and $\omega_0\sim 10\ \mathrm{s}^{-1}$. For these values most of the frequencies lie between $10\ \mathrm{s}^{-1}$ and $100\ \mathrm{s}^{-1}$, whenever stable oscillations exist.

For a general initial state near the trivial equilibrium point, which is $\Delta\varphi_{1,2}=0$ and $\Delta N_{1,2}=0$, the oscillations in

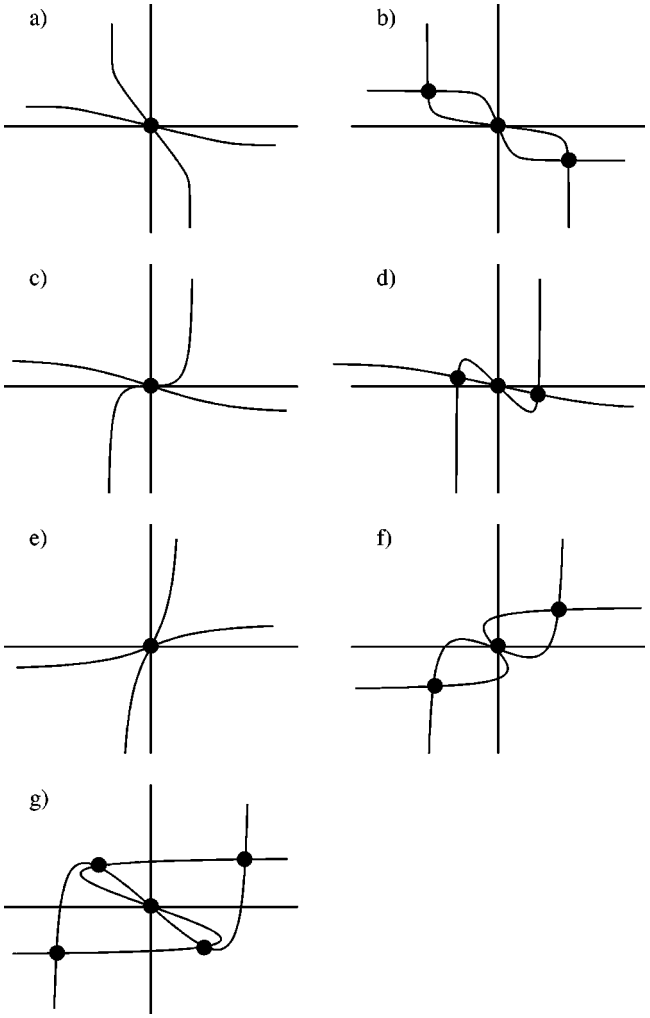

FIG. 3. Equations (A1) and (A2) plotted on the $(\Delta N_1, \Delta N_2)$ plane for different possible values of the relevant parameters. The intersection of the two curves is the graphical solution for the equilibrium points for $\Delta\varphi_1=\Delta\varphi_2=0$ (a),(b), $\Delta\varphi_1=\pi$ and $\Delta\varphi_2=0$ (c),(d), and $\Delta\varphi_1=\Delta\varphi_2=\pi$ (e)–(g). The criteria of applicability for the different figures are given in the Appendix.

$\Delta N_{1,2}$ and $\Delta\varphi_{1,2}$ will be a superposition of both density and spin modes. For the typical parameters that we are using, the frequency of the density mode is one order of magnitude larger than that of the spin mode and, therefore, it should be simple to distinguish between them experimentally. It should also be possible to prepare an initial state in which only one of the two modes is significantly excited.

Although π states are unstable in the spinless case for typical parameters, we have shown that they can be stabilized in spinor condensates. To prepare them experimentally we must have $N_1<N_2$ as explained in the Appendix, where the π phase difference is in species 1. A frequency measurement of the density mode could be used to detect that in fact a π phase exists in species 1. Alternatively, one could observe the destabilization of the state suddenly appearing in the form of density oscillations due to the reduction of N_2. Finally, a third possibility would be the direct imaging of the interference pattern between the left and right condensates of species 1 during its expansion, after the trapping potentials have been switched off.

In the spinless case the self-trapped π state occurs at the value $\Delta N^0=\sqrt{N^2-(\omega_0/\epsilon)^2}$. For the values of the parameters that we have assumed we get $\Delta N^0=N-o(1)$, which means that one of the sides of the junction is not macroscopically occupied, rendering the Gross-Pitaevskii description invalid. In the spinor case we see from Figs. 3(d)–3(f) that it is plausible that ΔN_i^0 is very close to N_i and we no longer expect our model to work in that region.

IV. $F=1$ SPIN JOSEPHSON EFFECT

In this section we look at the Hamiltonian, mean-field ground state, and oscillation modes of a Josephson junction containing atoms with $F=1$ total spin. We also study the stability of certain π states. The ground state of a single spinor condensate has been analyzed in the literature [6–9]. Here we extend the analysis to the case where the condensate is comprised of two spatially separated parts linked by a weak junction. Some of the results in this section are similar to those of Ref. [6] and are related to the bulk excitation spectrum of spin-1 condensates. As in the preceding sections we assume that the trapping potentials are identical for all three hyperfine states (which can be achieved using optical dipole traps). Under these conditions it is known that all three hyperfine states of the multiplet are miscible.

One might try to proceed as in Sec. III by deriving a set of equations for invariant quantities such as ΔN_+, α_+, β_+, and so on. However it turns out that while this is possible, it does not lead to simple equations of motion as in the two-internal-state system and therefore this approach does not seem to provide a clear insight into the dynamics.

We shall now study the small oscillations around some of the equilibrium points in both the ferromagnetic and antiferromagnetic cases,

$$H=H_J+H_{\rm int}, \tag{22}$$

where

$$H_J=-\frac{\omega_0}{2}\sum_i a_{i,L}^\dagger a_{i,R}+\text{H.c.}, \tag{23}$$

and (see [8])

$$\begin{aligned}H_{\rm int}=&\sum_{i=R,L}\frac{\epsilon_0}{4}(a_{1,i}^\dagger a_{1,i}^\dagger a_{1,i}a_{1,i}+a_{0,i}^\dagger a_{0,i}^\dagger a_{0,i}a_{0,i}\\&+a_{-1,i}^\dagger a_{-1,i}^\dagger a_{-1,i}a_{-1,i}+2a_{1,i}^\dagger a_{0,i}^\dagger a_{0,i}a_{1,i}\\&+2a_{0,i}^\dagger a_{-1,i}^\dagger a_{-1,i}a_{0,i}+2a_{1,i}^\dagger a_{-1,i}^\dagger a_{-1,i}a_{1,i})\\&+\frac{\epsilon_2}{4}(a_{1,i}^\dagger a_{1,i}^\dagger a_{1,i}a_{1,i}+a_{-1,i}^\dagger a_{-1,i}^\dagger a_{-1,i}a_{-1,i}\\&+2a_{1,i}^\dagger a_{0,i}^\dagger a_{0,i}a_{1,i}+2a_{0,i}^\dagger a_{-1,i}^\dagger a_{-1,i}a_{0,i}\\&-2a_{1,i}^\dagger a_{-1,i}^\dagger a_{-1,i}a_{1,i}+2a_{1,i}^\dagger a_{-1,i}^\dagger a_{0,i}a_{0,i}\\&+2a_{0,i}^\dagger a_{0,i}^\dagger a_{1,i}a_{-1,i}-a_{1,i}^\dagger a_{1,i}-a_{-1,i}^\dagger a_{-1,i}).\end{aligned} \tag{24}$$

For ^{23}Na and ^{87}Rb, ϵ_2 is a few percent of ϵ_0.

We now derive the equations of motion and, in the mean-field approximation, since we are assuming a macroscopic occupation, we linearize by keeping only terms at least of order N in $H_{\rm int}$.

For the ferromagnetic case, if we assume that only the $m_F=1$ has macroscopic occupation, we obtain the equations

$$\left(\mu+i\frac{d}{dt}\right)\begin{pmatrix}\delta\phi_{1,L}\\ \delta\phi_{0,L}\\ \delta\phi_{-1,L}\end{pmatrix}=-\frac{\omega_0}{2}\begin{pmatrix}\delta\phi_{1,R}\\ \delta\phi_{0,R}\\ \delta\phi_{-1,R}\end{pmatrix}+\frac{N}{2}\begin{pmatrix}\epsilon_0+\epsilon_2 & 0 & 0\\ 0 & \epsilon_0+\epsilon_2 & 0\\ 0 & 0 & \epsilon_0-\epsilon_2\end{pmatrix}\times\begin{pmatrix}2\delta\phi_{1,L}+\delta\phi_{1,L}^*\\ \delta\phi_{0,L}\\ \delta\phi_{-1,L}\end{pmatrix}, \tag{25}$$

and a similar set for $\delta\phi_{i,R}$. μ is the chemical potential given by

$$\mu=\mp\frac{\omega_0}{2}+\frac{\epsilon_0+\epsilon_2}{2}N, \tag{26}$$

where the upper and lower signs correspond to a 0 and π phase between the two condensates, respectively.

Solving them gives the following results: for the ground state (the relative phase between $\phi_{1,R}$ and $\phi_{1,L}$ equal to zero), we find a density mode with frequency $\sqrt{\omega_0^2+\omega_0(\epsilon_0+\epsilon_2)N}$, a spin mode with frequency ω_0, and a quadrupole mode with frequency $\omega_0+|\epsilon_2|N$.

For the π state we find the same modes with frequencies $\sqrt{\omega_0^2-\omega_0(\epsilon_0+\epsilon_2)N}$, $-\omega_0$, and $-\omega_0+|\epsilon_2|N$. The density mode can clearly become unstable for $\omega_0<(\epsilon_0+\epsilon_2)N$, which is the case for the typical parameters quoted in the preceding section. The two modes with negative frequencies are dynamically stable but thermodynamically unstable, i.e., in the presence of dissipation this equilibrium point becomes unstable.

For the antiferromagnetic case, if we assume that only the $m_F=0$ state is macroscopically occupied, we obtain the equations

$$\left(\mu+i\frac{d}{dt}\right)\begin{pmatrix}\delta\phi_{1,L}\\ \delta\phi_{0,L}\\ \delta\phi_{-1,L}\end{pmatrix}=-\frac{\omega_0}{2}\begin{pmatrix}\delta\phi_{1,R}\\ \delta\phi_{0,R}\\ \delta\phi_{-1,R}\end{pmatrix}+\frac{N}{2}\begin{pmatrix}\epsilon_0+\epsilon_2 & 0 & 0\\ 0 & \epsilon_0 & 0\\ 0 & 0 & \epsilon_0+\epsilon_2\end{pmatrix}\times\begin{pmatrix}\delta\phi_{1,L}\\ 2\delta\phi_{0,L}+\delta\phi_{0,L}^*\\ \delta\phi_{-1,L}\end{pmatrix}+\frac{N\epsilon_2}{2}\begin{pmatrix}\delta\phi_{-1,L}^*\\ 0\\ \delta\phi_{1,L}^*\end{pmatrix}, \tag{27}$$

and a similar set for $\delta\phi_{i,R}$. The chemical potential μ is given by Eq. (26) with ϵ_0 replacing $(\epsilon_0+\epsilon_2)$.

Solving them gives the following results. For the ground state (the relative phase between $\phi_{0,R}$ and $\phi_{0,L}$ equal to zero), we have the following three modes: a density mode with frequency $\sqrt{\omega_0^2+\omega_0\epsilon_0N}$ and two degenerate spin modes with frequency $\sqrt{\omega_0^2+\omega_0\epsilon_2N}$.

For the π state we find the same modes with frequencies $\sqrt{\omega_0^2-\omega_0\epsilon_0N}$ and $\sqrt{\omega_0^2-\omega_0\epsilon_2N}$. The density mode becomes unstable for $\omega_0<\epsilon_0N$ and the spin modes become unstable for $\omega_0<\epsilon_2N$. With the parameters that we are using, at the very least the density mode is unstable.

V. CONCLUSIONS

We have considered the Josephson junction between two spatially separated condensates with a hyperfine degree of freedom. We have derived a set of simple equations which, in the isotropic limit, are formally identical to the Bloch equations and which provide insight into the dynamics of the two-hyperfine-state condensate in a double-well setup. We find a partial mapping to the simple problem of a particle in a $(\pm x^2+x^4)$-type potential, which becomes a complete mapping in the spinless case. We have also demonstrated the existence in this system of density and spin oscillation modes. In particular, we have found π states that are stable under experimentally accessible conditions due to the interactions between the two species. Finally we analyzed the spin-1 case in the same geometry both for the ferromagnetic and antiferromagnetic cases and found the low-lying oscillation modes. Our results indicate a wide range of phenomenology for Josephson oscillations when the superfluid has a spin degree of freedom. Future possible directions of research might include tunneling between fragmented states [23] and more general solutions of the Bloch equations.

ACKNOWLEDGMENTS

We would like to thank A. J. Leggett for many insightful comments and especially for drawing our attention to this problem. We would also like to thank N. Hatakenaka and I. Zapata for several stimulating discussions. Additionally we received useful advice from G. Baym, Y. Castin, S. Kurihara, E. Mueller, and G. S. Paraoanu. This work was supported by the NSF Grant No. DMR99-86199. C.L. acknowledges FCT (Portugal) for support. S.A. would like to thank N. Hatakenaka and H. Takayanagi for their hospitality during his stay at NTT Basic Research Laboratories and acknowledges support from NTT Corporation.

APPENDIX: CALCULATION OF EQUILIBRIUM POINTS AND OSCILLATION FREQUENCIES FOR THE TWO-COMPONENT CASE

At an equilibrium point, $\dot{\Delta N}_{1,2}=\dot{\Delta\varphi}_{1,2}=0$. Using Eq. (5) this implies that the phases $\Delta\varphi_1$ and $\Delta\varphi_2$ are either zero or π. From Eq. (6) we get

$$\Delta N_1^0 = -\Delta N_2^0 \left(\frac{\epsilon_{22}}{\epsilon_{12}} + \frac{\omega_0}{\epsilon_{12}\sqrt{N_2^2-(\Delta N_2^0)^2}\zeta_2} \right), \quad \text{(A1)}$$

$$\Delta N_2^0 = -\Delta N_1^0 \left(\frac{\epsilon_{11}}{\epsilon_{12}} + \frac{\omega_0}{\epsilon_{12}\sqrt{N_1^2-(\Delta N_1^0)^2}\zeta_1} \right), \quad \text{(A2)}$$

where ΔN_i^0 and $\Delta\varphi_i^0$ are the coordinates of the equilibrium point. We have defined $\zeta_1 \equiv \cos\Delta\varphi_1^0$ and $\zeta_2 \equiv \cos\Delta\varphi_2^0$ to abbreviate the formulas.

These equations define two functions, $\Delta N_1^0(\Delta N_2^0)$ and $\Delta N_2^0(\Delta N_1^0)$, which we can plot on the $(\Delta N_1^0, \Delta N_2^0)$ plane (Fig. 3). Since both ζ_1 and ζ_2 can be 1 or -1 (corresponding to $\Delta\varphi_i^0 = 0$ or π) we have three distinct cases. For all of them the trivial point $\Delta N_1^0 = \Delta N_2^0 = 0$ is always a solution. Therefore in all cases we have at least one solution.

a. Case 1. $\zeta_1 = \zeta_2 = 1$ $(\Delta\varphi_1 = \Delta\varphi_2 = 0)$

As is clear from Figs. 3(a) and 3(b), the condition for the existence of three solutions imposes a condition on the slopes of the curves at the origin, which leads to

$$\left(\frac{\epsilon_{22}}{\epsilon_{12}} + \frac{\omega_0}{\epsilon_{12}N_2} \right)\left(\frac{\epsilon_{11}}{\epsilon_{12}} + \frac{\omega_0}{\epsilon_{12}N_1} \right) < 1. \quad \text{(A3)}$$

b. Case 2. $\zeta_1 = -1$, $\zeta_2 = 1$ $(\Delta\varphi_1 = \pi, \Delta\varphi_2 = 0)$

For three solutions to exist [Figs. 3(c) and 3(d)], we require this time that

$$\left(\frac{\epsilon_{11}}{\epsilon_{12}} - \frac{\omega_0}{\epsilon_{12}N_1} \right)\left(\frac{\epsilon_{22}}{\epsilon_{12}} + \frac{\omega_0}{\epsilon_{12}N_2} \right) > 1. \quad \text{(A4)}$$

c. Case 3: $\zeta_1 = \zeta_2 = -1$ $(\Delta\varphi_1 = \Delta\varphi_2 = \pi)$

This time we may have one [Fig. 3(e)], three [Fig. 3(f)], or five [Fig. 3(g)] solutions. To have three we need that

$$\left(\frac{\epsilon_{22}}{\epsilon_{12}} - \frac{\omega_0}{\epsilon_{12}N_2} \right)\left(\frac{\epsilon_{11}}{\epsilon_{12}} - \frac{\omega_0}{\epsilon_{12}N_1} \right) < 1. \quad \text{(A5)}$$

If this condition is not met, we will have one or five solutions, depending on whether the factors on the left-hand side are both negative or both positive, respectively.

In the rest of this appendix we will analyze the behavior of the system close to the various equilibrium points. Notice that the global ground state is the trivial solution $\Delta N_{1,2} = 0$ and $\Delta\varphi_{1,2} = 0$. All the other equilibrium points are thermodynamically unstable although possibly dynamically stable [22].

1. Isotropic case

If all ϵ_{ij}'s are equal then some of the conditions above cannot be satisfied. For case 1, condition (A3) cannot be satisfied and therefore only the equilibrium point $\Delta N_1 = \Delta N_2 = 0$ is allowed.

In case 2 both single and triple solutions are allowed. Condition (A4) for the existence of three equilibrium points becomes $N_1 - N_2 - \omega_0/\epsilon > 0$.

In case 3 the conditions for the existence of one or three equilibrium points can be satisfied. The condition for three is $N_1 + N_2 - \omega_0/\epsilon > 0$. However we cannot have five equilibrium points since if both terms are positive in condition (A5) and each of them is smaller than 1, their product will also be smaller than 1.

To study the behavior in the neighborhood of an equilibrium point we shall work with the second-order differential equations for ΔN_1 and ΔN_2. To obtain these we differentiate Eq. (5) with respect to time and eliminate $\dot{\Delta\varphi}_{1,2}$ and $\dot{\Delta N}_{1,2}$ using Eqs. (5) and (6). We now introduce the variables δ_1, δ_2 defined by

$$\Delta N_1 = \Delta N_1^0 + \delta_1, \quad \text{(A6)}$$

$$\Delta N_2 = \Delta N_2^0 + \delta_2. \quad \text{(A7)}$$

The linearized equations of motion for the isotropic case are

$$\begin{pmatrix} \ddot{\delta}_1 \\ \ddot{\delta}_2 \end{pmatrix} = -\mathbf{\Omega}^2 \begin{pmatrix} \delta_1 \\ \delta_2 \end{pmatrix}, \quad \text{(A8)}$$

where

$$\mathbf{\Omega}^2 = (\omega_0^2 + \epsilon^2(\Delta N_+^0)^2)\mathbf{Id} + \omega_0\epsilon \begin{pmatrix} \sqrt{N_1^2-(\Delta N_1^0)^2}\zeta_1 & \sqrt{N_1^2-(\Delta N_1^0)^2}\zeta_1 \\ \sqrt{N_2^2-(\Delta N_2^0)^2}\zeta_2 & \sqrt{N_2^2-(\Delta N_2^0)^2}\zeta_2 \end{pmatrix}. \quad \text{(A9)}$$

a. Case 1: $\zeta_1 = \zeta_2 = 1$

As mentioned before, the only stable point is at $\Delta N_1^0 = \Delta N_2^0 = 0$. In the basis (δ_1, δ_2) we find the modes (N_1, N_2) and $(1, -1)$ (note that the matrix of the linearized equations of motion is not Hermitian and therefore the two eigenvectors are not guaranteed to be orthogonal even if the corresponding frequencies are different). The first corresponds to a density mode with frequency $\sqrt{\omega_0^2 + \omega_0\epsilon N}$ and the second to a spin mode with frequency ω_0. Note though that, even in the density mode, the total spin on each side of the junction changes as a function of time (unless $N_1 = N_2$).

b. Case 2. $\zeta_1 = -1$, $\zeta_2 = 1$

Near $\Delta N_1^0 = \Delta N_2^0 = 0$ we proceed as above and find the eigenfrequencies $\sqrt{\omega_0^2 + \omega_0\epsilon(N_2 - N_1)}$ and ω_0 with corresponding eigenvectors $(N_1, -N_2)$ and $(1, -1)$. The system is dynamically stable as long as the frequencies are real, which leads to the condition $N_1 - N_2 - \omega_0/\epsilon < 0$. Since N_1 and N_2 are easy to change experimentally, this state can always be made stable regardless of the values of ω_0 and ϵ. It is therefore much easier to obtain a π state this way than in the spinless case. However there is an additional complication: if $N_1 = N_2$, the eigenvectors become parallel and, since the representation of arbitrary vectors in an almost collinear

basis can involve very large amplitudes (especially for the vectors perpendicular to the basis vectors), the amplitude of the oscillations for initial displacements in the in-phase direction will tend to diverge as $(N_2-N_1)/N\to 0$ after some time. Experimentally it is not difficult to avoid this pitfall. Near the equilibrium point $\Delta N_1^0\neq 0$ and $\Delta N_2^0\neq 0$ the frequencies become $\epsilon|\Delta N_+^0|$ for the density mode and $\sqrt{\omega_0^2+\epsilon^2(\Delta N_+^0)^2}$ for the spin mode. Both frequencies are real and therefore this equilibrium point is stable (however, see Sec. III D).

c. Case 3. $\zeta_1=\zeta_2=-1$

For $\Delta N_1^0=\Delta N_2^0=0$ we find the eigenfrequencies $\sqrt{\omega_0^2-\omega_0\epsilon N}$ and ω_0 with corresponding eigenvectors (N_1,N_2) and $(1,-1)$. The system is dynamically stable as long as $N<\omega_0/\epsilon$. For $\Delta N_1^0,\Delta N_2^0\neq 0$ the frequencies of the two eigenmodes are given by the same expressions as those for $\Delta N_1^0,\Delta N_2^0\neq 0$ in case 2 [$\epsilon|\Delta N_+^0|$ and $\sqrt{\omega_0^2+\epsilon^2(\Delta N_+^0)^2}$] and therefore they are both stable as long as the points exist.

Note that all the frequencies found in Sec. III A are in agreement with those derived here by studying the small oscillation behavior directly from Eqs. (5) and (6).

2. Anisotropic case

In the anisotropic case we can still use Eq. (A8) but with $\mathbf{\Omega}^2$ given by

$$\mathbf{\Omega}^2=\begin{pmatrix}\omega_0^2+(\epsilon_{11}\Delta N_1^0+\epsilon_{12}\Delta N_2^0)^2 & 0\\ 0 & \omega_0^2+(\epsilon_{22}\Delta N_2^0+\epsilon_{12}\Delta N_1^0)^2\end{pmatrix}+\omega_0\begin{pmatrix}\epsilon_{11}\sqrt{N_1^2-(\Delta N_1^0)^2}\zeta_1 & \epsilon_{12}\sqrt{N_1^2-(\Delta N_1^0)^2}\zeta_1\\ \epsilon_{12}\sqrt{N_2^2-(\Delta N_2^0)^2}\zeta_2 & \epsilon_{22}\sqrt{N_2^2-(\Delta N_2^0)^2}\zeta_2\end{pmatrix}. \tag{A10}$$

a. Case 1. $\zeta_1=\zeta_2=1$

When $\Delta N_1^0=\Delta N_2^0=0$ the eigenvalues are

$$\omega^2=\omega_0^2+\omega_0\left(\frac{\epsilon_{11}N_1\zeta_1+\epsilon_{22}N_2\zeta_2}{2}\pm\sqrt{\frac{(\epsilon_{11}N_1\zeta_1-\epsilon_{22}N_2\zeta_2)^2}{4}+\epsilon_{12}^2N_1N_2\zeta_1\zeta_2}\right) \tag{A11}$$

with $\zeta_1=\zeta_2=1$. For simplicity we shall address only the nearly isotropic case. It is experimentally relevant since this is the case for both ^{23}Na and ^{87}Rb, where the experimental values for the $\epsilon_{11},\epsilon_{22}$, and ϵ_{12} are similar. To do this we use the variables $\epsilon,\epsilon_{A,B}$ defined in Sec. III B, since ϵ_A and ϵ_B quantify the degree of anisotropy. We therefore treat them as small parameters. Expanding the square root in Eq. (A11) and keeping terms to first order in those variables we obtain the two eigenvalues

$$\omega^2=\omega_0^2+\omega_0\epsilon(N_1\zeta_1+N_2\zeta_2)+\omega_0\epsilon_A\frac{(N_1\zeta_1-N_2\zeta_2)^2}{N_1\zeta_1+N_2\zeta_2}+2\omega_0\epsilon_B(N_1\zeta_1-N_2\zeta_2), \tag{A12}$$

$$\omega^2=\omega_0^2+4\omega_0\epsilon_A\frac{N_1N_2\zeta_1\zeta_2}{N_1\zeta_1+N_2\zeta_2}. \tag{A13}$$

We have assumed that $N_1+N_2\sim N_1-N_2\sim N$. Since $\epsilon_A>0$ (which is implied by the miscibility condition) both modes are stable ($\epsilon_B\ll\epsilon$). The instability that would arise at sufficiently large and negative values of ϵ_A has the same origin as the immiscibility condition. However, we do not consider this region in this paper since immiscibility would have severe consequences (see end of Sec. II). It is easy to see from Eq. (A3) that the case $\Delta N_1^0,\Delta N_2^0\neq 0$ is also ruled out due to the miscibility condition.

b. Case 2. $\zeta_1=-1,\zeta_2=1$

At the origin $\Delta N_1^0=\Delta N_2^0=0$ the frequencies are again given by Eqs. (A12) and (A13) but with $\zeta_1=-1,\zeta_2=1$. Let us divide the region into two parts: $N_1-N_2>0$ and $N_1-N_2<0$. In the first region the motion is always unstable: for large values of N_1-N_2 the first frequency is imaginary, and for small values the resonance of Sec. IV A will tend to destabilize the equilibrium point. In the second region, if $N_1-N_2>-4\epsilon_AN_1N_2/\omega_0$ then again it is unstable. Otherwise it is stable (provided it is outside the region of resonance). For $\Delta N_1^0,\Delta N_2^0\neq 0$, the conditions for stability become rather complex and offer little insight. However, it is reasonable to believe that, by suitably choosing the parameters, most of the equilibrium points can be made stable (here also, see caution in Sec. III D).

c. Case 3. $\zeta_1=\zeta_2=-1$

The frequencies at the point $\Delta N_1^0=\Delta N_2^0=0$ are those given by Eqs. (A12) and (A13) with $\zeta_1=\zeta_2=-1$. As in the isotropic case, the point $\Delta N_1^0=\Delta N_2^0=0$ is unstable for typical experimental conditions, namely, when $\epsilon N>\omega_0$. The corrections to this criterion are of order $(\epsilon_A,\epsilon_B)/\epsilon$. Finally, when $\Delta N_1^0,\Delta N_2^0\neq 0$, as in the preceding case, the stability can generally be achieved for all equilibrium points for appropriate values of the parameters, barring immiscibility problems.

[1] S. Backhaus, S. Pereverzev, R. W. Simmonds, A. Loshak, J. C. Davis, and R. E. Packard, Nature (London) **398**, 687 (1998).
[2] S.-K. Yip, Phys. Rev. Lett. **83**, 3864 (1999).
[3] J. K. Viljas and E. V. Thuneberg, Phys. Rev. Lett. **83**, 3868 (1999).
[4] C. J. Myatt, E. A. Burt, R. W. Ghrist, E. A. Cornell, and C. E. Wieman, Phys. Rev. Lett. **78**, 586 (1997).
[5] D. M. Stamper-Kurn, M. R. Andrews, A. P. Chikkatur, S. Inouye, H.-J. Miesner, J. Stenger, and W. Ketterle, Phys. Rev. Lett. **80**, 2027 (1998).
[6] T. L. Ho, Phys. Rev. Lett. **81**, 742 (1998).
[7] T. Ohmi and K. Machida, J. Phys. Soc. Jpn. **67**, 1822 (1998).
[8] C. K. Law, H. Pu, and N. P. Bigelow, Phys. Rev. Lett. **81**, 5257 (1998).
[9] M. Koashi and M. Ueda, Phys. Rev. Lett. **84**, 1066 (2000).
[10] S. Giovanazzi, A. Smerzi, and S. Fantoni, Phys. Rev. Lett. **84**, 4521 (2000).
[11] A. Smerzi, S. Fantoni, S. Giovanazzi, and S. R. Shenoy, Phys. Rev. Lett. **79**, 4950 (1997); S. Raghavan, A. Smerzi, S. Fantoni, and S. R. Shenoy, Phys. Rev. A **59**, 620 (1999).
[12] G. J. Milburn, J. Corney, E. M. Wright, and D. F. Walls, Phys. Rev. A **55**, 4318 (1997).
[13] J. Ruostekoski and D. F. Walls, Phys. Rev. A **58**, R50 (1998).
[14] P. Villain and M. Lewenstein, Phys. Rev. A **59**, 2250 (1999).
[15] I. Zapata, F. Sols, and A. J. Leggett, Phys. Rev. A **57**, R28 (1998).
[16] J. Williams, R. Walser, J. Cooper, E. Cornell, and M. Holland, Phys. Rev. A **59**, R31 (1999).
[17] A. J. Leggett, Rev. Mod. Phys. **73**, 307 (2001).
[18] B. P. Anderson and M. A. Kasevich, Science **282**, 1686 (1998).
[19] F. S. Cataliotti, S. Burger, C. Fort, P. Maddaloni, F. Minardi, A. Trombettoni, A. Smerzi, and M. Inguscio, Science **293**, 843 (2001).
[20] J. Williams, R. Walser, J. Cooper, E. Cornell, and M. Holland, Phys. Rev. A **59**, R31 (1999).
[21] T. L. Ho and V. B. Shenoy, Phys. Rev. Lett. **77**, 3276 (1996). It is known that the $|F=2,m_F=1\rangle$ and $|F=1,m_F=-1\rangle$ hyperfine states of ^{87}Rb are miscible (see, e.g., [4]).
[22] For a discussion of thermodynamic vs dynamic stability, see, e.g., Y. Castin and R. Dum, Eur. Phys. J. D **7**, 399 (1999).
[23] M. Oktel and T. L. Ho (unpublished).